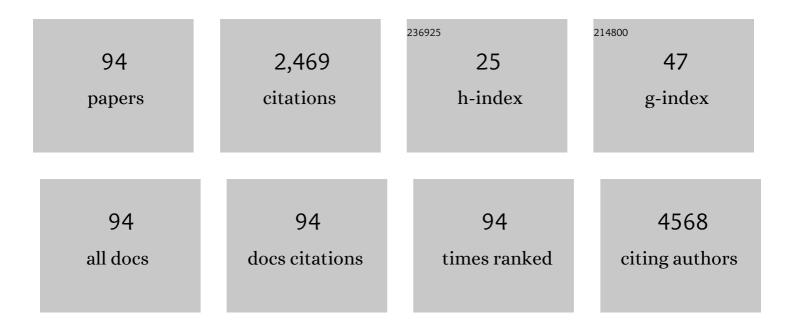
List of Publications by Year in descending order

Source: https://exaly.com/author-pdf/4504851/publications.pdf Version: 2024-02-01



Υίν Ζηλνς

#	Article	IF	CITATIONS
1	Mechanism of regulation of stem cell differentiation by matrix stiffness. Stem Cell Research and Therapy, 2015, 6, 103.	5.5	287
2	Thermally Stable, Biocompatible, and Flexible Organic Fieldâ€Effect Transistors and Their Application in Temperature Sensing Arrays for Artificial Skin. Advanced Functional Materials, 2015, 25, 2138-2146.	14.9	184
3	Large Magnetostriction from Morphotropic Phase Boundary in Ferromagnets. Physical Review Letters, 2010, 104, 197201.	7.8	148
4	Ultrasensitive Photodetectors Based on Island-Structured CH ₃ NH ₃ PbI ₃ Thin Films. ACS Applied Materials & Interfaces, 2015, 7, 21634-21638.	8.0	108
5	Preparation and <i>in vitro</i> / <i>in vivo</i> evaluation of resveratrol-loaded carboxymethyl chitosan nanoparticles. Drug Delivery, 2016, 23, 971-981.	5.7	95
6	Robust ferromagnetism in Mn-doped MoS2 nanostructures. Applied Physics Letters, 2016, 109, .	3.3	91
7	Co3O4–carbon nanotube heterostructures with bead-on-string architecture for enhanced lithium storage performance. Nanoscale, 2013, 5, 8067.	5.6	78
8	Enhancement of solubility, antioxidant ability and bioavailability of taxifolin nanoparticles by liquid antisolvent precipitation technique. International Journal of Pharmaceutics, 2014, 471, 366-376.	5.2	77
9	Functionalization-assistant ball milling towards Si/graphene anodes in high performance Li-ion batteries. Carbon, 2021, 181, 300-309.	10.3	74
10	A Beaded-String Silicon Anode. ACS Nano, 2013, 7, 2717-2724.	14.6	68
11	Noncubic crystallographic symmetry of a cubic ferromagnet: Simultaneous structural change at the ferromagnetic transition. Physical Review B, 2008, 77, .	3.2	67
12	Confined propagation of covalent chemical reactions on single-walled carbon nanotubes. Nature Communications, 2011, 2, 382.	12.8	67
13	Electrospun hollow cage-like α-Fe ₂ O ₃ microspheres: synthesis, formation mechanism, and morphology-preserved conversion to Fe nanostructures. CrystEngComm, 2014, 16, 10618-10623.	2.6	63
14	Preparation and characterization of paclitaxel nanosuspension using novel emulsification method by combining high speed homogenizer and high pressure homogenization. International Journal of Pharmaceutics, 2015, 490, 324-333.	5.2	59
15	Facile Synthesis of a MoS ₂ and Functionalized Graphene Heterostructure for Enhanced Lithium-Storage Performance. ACS Applied Materials & Interfaces, 2017, 9, 12907-12913.	8.0	56
16	Controlled Defects in Semiconducting Carbon Nanotubes Promote Efficient Generation and Luminescence of Trions. ACS Nano, 2014, 8, 4239-4247.	14.6	52
17	Propagative Sidewall Alkylcarboxylation that Induces Red-Shifted Near-IR Photoluminescence in Single-Walled Carbon Nanotubes. Journal of Physical Chemistry Letters, 2013, 4, 826-830.	4.6	46
18	Effect of superfine grinding on physicochemical and antioxidant properties of pomegranate peel. International Journal of Food Science and Technology, 2016, 51, 212-221.	2.7	45

YIN ZHANG

15

#	Article	IF	CITATIONS
19	CuO Necklace: Controlled Synthesis of a Metal Oxide and Carbon Nanotube Heterostructure for Enhanced Lithium Storage Performance. Journal of Physical Chemistry C, 2013, 117, 12346-12351.	3.1	42
20	Molten hydroxides synthesis of hierarchical cobalt oxide nanostructure and its application as anode material for lithium ion batteries. Electrochimica Acta, 2011, 56, 4876-4881.	5.2	41
21	Giant spontaneous exchange bias triggered by crossover of superspin glass in Sb-doped Ni50Mn38Ga12 Heusler alloys. Scientific Reports, 2016, 6, 30801.	3.3	40
22	Preparation and characterization of micronized ellagic acid using antisolvent precipitation for oral delivery. International Journal of Pharmaceutics, 2015, 486, 207-216.	5.2	34
23	Lithium-assisted exfoliation of pristine graphite for few-layer graphene nanosheets. Nano Research, 2015, 8, 801-807.	10.4	34
24	Evidence for first-order nature of the ferromagnetic transition in Ni, Fe, Co, and <mml:math xmlns:mml="http://www.w3.org/1998/Math/MathML" display="inline"><mml:mrow><mml:msub><mml:mrow><mml:mtext>CoFe</mml:mtext></mml:mrow><mml:m Physical Review B, 2008, 78, .</mml:m </mml:msub></mml:mrow></mml:math 	n>23:7mml	:mñ?
25	Interfacial Mechanics of Carbon Nanotube@Amorphousâ€Si Coaxial Nanostructures. Advanced Materials, 2011, 23, 4318-4322.	21.0	26
26	Diameter-dependent, progressive alkylcarboxylation of single-walled carbon nanotubes. Chemical Communications, 2011, 47, 758-760.	4.1	24
27	Isolation and Functional Characterization of a Lycopene β-cyclase Gene Promoter from Citrus. Frontiers in Plant Science, 2016, 7, 1367.	3.6	24
28	Transmittance Tunable Smart Window Based on Magnetically Responsive 1D Nanochains. ACS Applied Materials & Interfaces, 2020, 12, 31637-31644.	8.0	23
29	The high water solubility of inclusion complex of taxifolin-γ-CD prepared and characterized by the emulsion solvent evaporation and the freeze drying combination method. International Journal of Pharmaceutics, 2014, 477, 148-158.	5.2	22
30	Machine Learning Magnetic Parameters from Spin Configurations. Advanced Science, 2020, 7, 2000566.	11.2	22
31	Molecular characterization, critical amino acid identification, and promoter analysis of a lycopene β-cyclase gene from citrus. Tree Genetics and Genomes, 2016, 12, 1.	1.6	18
32	Solubility and dissolution rate improvement of the inclusion complex of apigenin with 2-hydroxypropyl-β-cyclodextrin prepared using the liquid antisolvent precipitation and solvent removal combination methods. Drug Development and Industrial Pharmacy, 2017, 43, 1366-1377.	2.0	18
33	Highly Sensitive Mechanoresponsive Smart Windows Driven by Shear Strain. Advanced Functional Materials, 2021, 31, 2102350.	14.9	17
34	Magnetocaloric effect in the vicinity of the magnetic phase transition in <mml:math xmlns:mml="http://www.w3.org/1998/Math/MathML"> <mml:mrow> <mml:msub> <mml:mi> NdCo </mml:mi> <mi compounds. Physical Review B, 2020, 101, .</mi </mml:msub></mml:mrow></mml:math 	നി:ജമായ> <	:m nd: mn>2<
35	Electric modulation of conduction in multiferroic Ni-doped GaFeO ₃ ceramics. Journal Physics D: Applied Physics, 2018, 51, 225002.	2.8	15

Modification of Carbon Nanotubes via Birch Reaction for Enhanced HER Catalyst by Constructing
Pearl Necklaceâ€Like NiCo₂P₂â€"CNT Composite. Small, 2018, 14, e1804388.

YIN ZHANG

#	Article	IF	CITATIONS
37	A magnetocaloric effect arising from a ferromagnetic transition in the martensitic state in Heusler alloy of Ni50Mn36Sb8Ga6. Applied Physics Letters, 2015, 107, .	3.3	14
38	Preparation, characterization and bioavailability of oral puerarin nanoparticles by emulsion solvent evaporation method. RSC Advances, 2016, 6, 69889-69901.	3.6	14
39	Ursolic acid nanoparticles for oral delivery prepared by emulsion solvent evaporation method: characterization, <i>in vitro</i> evaluation of radical scavenging activity and bioavailability. Artificial Cells, Nanomedicine and Biotechnology, 2019, 47, 609-620.	2.8	14
40	Enhancement of the exchange coupling interaction of nanocomposite Nd2Fe14B/α-Fe magnets by a small amount of Sm substitution for Nd. Journal of Alloys and Compounds, 2005, 394, 1-4.	5.5	13
41	Enhanced dissolution rate and oral bioavailability of ginkgo biloba extract by preparing nanoparticles via emulsion solvent evaporation combined with freeze drying (ESE-FR). RSC Advances, 2016, 6, 77346-77357.	3.6	13
42	Dynamic Refractive Indexâ€Matching for Adaptive Thermoresponsive Smart Windows. Small, 2022, 18, .	10.0	13
43	Seed-mediated approach for the size-controlled synthesis of flower-like Ag mesostructures. Materials Letters, 2014, 130, 9-13.	2.6	12
44	Hierarchical Ag mesostructures for single particle SERS substrate. Applied Surface Science, 2017, 393, 197-203.	6.1	12
45	A facile strategy for Co3O4/Co nanoparticles encapsulated in porous N-doped carbon nanofibers towards enhanced lithium storage performance. Journal of Porous Materials, 2020, 27, 1-9.	2.6	12
46	Thermally reshaped polyvinylpyrrolidone/SnO2@p-toluenesulfonic acid-doped polypyrrole nanocables with high capacity and excellent cycle performance as anode for lithium-ion batteries. Journal of Alloys and Compounds, 2021, 867, 159067.	5.5	12
47	Gold-Substrate-Enhanced Scanning Electron Microscopy of Functionalized Single-Wall Carbon Nanotubes. Journal of Physical Chemistry Letters, 2011, 2, 885-888.	4.6	11
48	Enhanced multiferroic properties of lead-free (1-x)GaFeO3-(x)Co0.5Zn0.5Fe2O4 composites. Journal of Applied Physics, 2018, 124, .	2.5	11
49	Magnetocaloric effect and critical exponent analysis around magnetic phase transition in NdCo2 compound. Journal Physics D: Applied Physics, 2020, 53, 345003.	2.8	11
50	Fabrication of N, S co-doped carbon nanofiber matrix with cobalt sulfide nanoparticles enhancing lithium/sodium storage performance. Journal of Alloys and Compounds, 2022, 902, 163812.	5.5	11
51	A facile two-step approach to synthesize monodisperse and high-magnetization Fe3O4@PS composite colloidal particles for constructing dual-response photonic crystals. Composites Communications, 2020, 19, 114-120.	6.3	9
52	High temperature spin-glass-like transition in La _{0.67} Sr _{0.33} MnO ₃ nanofibers near the Curie point. Physical Chemistry Chemical Physics, 2017, 19, 16731-16736.	2.8	8
53	Long-Term Behaviour of Precast Concrete Deck Using Longitudinal Prestressed Tendons in Composite I-Girder Bridges. Applied Sciences (Switzerland), 2018, 8, 2598.	2.5	8
54	Zero-thermal-hysteresis magnetocaloric effect induced by magnetic transition at a morphotropic phase boundary in Heusler Ni ₅₀ Mn ₃₆ Sb _{14â^'x} In _x alloys. Physical Chemistry Chemical Physics, 2018, 20, 18484-18490.	2.8	8

#	Article	IF	CITATIONS
55	Improved magnetostriction in Galfenol alloys by aligning crystal growth direction along easy magnetization axis. Scientific Reports, 2020, 10, 20055.	3.3	8
56	Magnetocaloric effect in Tb(Co0.94Fe0.06)2 alloy with negligible thermal hysteresis and wide working temperature range. Journal of Magnetism and Magnetic Materials, 2020, 502, 166521.	2.3	8
57	Tailoring exchange bias in reentrant spin glass by ferromagnetic cluster size engineering. APL Materials, 2021, 9, .	5.1	8
58	Synthesis of monodisperse ferromagnetic CoxFe3â^'xO4 colloidal particles with magnetically tunable optical properties. CrystEngComm, 2019, 21, 2310-2319.	2.6	7
59	The Phase Diagram and Exotic Magnetostrictive Behaviors in Spinel Oxide Co(Fe1â^'xAlx)2O4 System. Materials, 2019, 12, 1685.	2.9	7
60	Spongy <i>p</i> -Toluenesulfonic Acid-doped Polypyrrole with Extraordinary Rate Performance as Durable Anodes of Sodium-Ion Batteries at Different Temperatures. Langmuir, 2020, 36, 15075-15081.	3.5	7
61	Magnetostructural transition, magnetocaloric effect and critical exponent analysis in Nd(Co0.8Fe0.2)2 alloy. Journal of Alloys and Compounds, 2022, 895, 162562.	5.5	7
62	Modeling magnetic nanotubes using a chain of ellipsoid-rings approach. Journal of Applied Physics, 2012, 111, 063912.	2.5	6
63	Functionalization of carbon nanotubes via Birch reduction chemistry for selective loading of CuO nanosheets. New Journal of Chemistry, 2015, 39, 4278-4283.	2.8	5
64	Temperature dependent magnetization and coercivity in morphotropic phase boundary involved ferromagnetic Tb1-xGdxFe2 system. Materials Chemistry and Physics, 2018, 217, 278-284.	4.0	5
65	Spin cluster size dependence of exchange bias effect in Mn50Ni40Ga10 Heusler alloys. Intermetallics, 2019, 107, 10-14.	3.9	5
66	Gramâ€5cale Production of Graphene Powder via a Quasiâ€physical Process and Its Application in Electrode Material for Lithiumâ€Ion Battery. Advanced Engineering Materials, 2019, 21, 1800891.	3.5	5
67	The promising room-temperature magnetic refrigeration materials — Misch-metal (MM)2Fe17-xSix (x=0–1.5) compounds. Journal of Alloys and Compounds, 2020, 828, 154404.	5.5	5
68	SnO2@C nanowires as high-performance anodic materials for lithium-ion batteries. Materials Letters, 2021, 284, 129019.	2.6	5
69	Photo-controlled exchange bias in CoO@Co–Fe PBA core–shell heterostructures. Journal of Materials Chemistry C, 2021, 10, 244-250.	5.5	5
70	Large magnetocaloric effect and near-zero thermal hysteresis in the rare earth intermetallic Tb1â^'x Dy x Co2 compounds. Journal of Physics Condensed Matter, 2017, 29, 055804.	1.8	4
71	Three-dimensional nanocomposites with Co ₃ O ₄ nanosheets parallelly embedded in carbon network walls for enhanced lithium-ion storage. Dalton Transactions, 2019, 48, 8375-8383.	3.3	4
72	Giant exchange bias induced <i>via</i> tuning interfacial spins in polycrystalline Fe ₃ O ₄ /CoO bilayers. Physical Chemistry Chemical Physics, 2021, 23, 4805-4810.	2.8	4

#	Article	IF	CITATIONS
73	Maximizing Zero-Field-Cooled Exchange Bias in Crystallized Co@CoO Nanocluster Assembled Thin Film by Varying Film Thickness. Journal of Physical Chemistry C, 2021, 125, 7337-7342.	3.1	4
74	Understanding of the giant magnetic entropy change around the co-occurrence point of martensitic and magnetic transitions in Ni-Mn-In Heusler alloy. Acta Materialia, 2022, 229, 117839.	7.9	4
75	Single Capillary Electrospinning of Magnetic Core-shell Nanofibers. ChemistrySelect, 2016, 1, 1510-1514.	1.5	3
76	Novel cucurbitane-type triterpene saponins from <i>Hemsleya amabilis</i> . Journal of Asian Natural Products Research, 2020, 22, 30-37.	1.4	3
77	Simulating magnetic nanotubes using a chain of ellipsoid-rings model with a magnetization reversal process by fanning rotation. Physical Chemistry Chemical Physics, 2015, 17, 10250-10256.	2.8	2
78	Stepwise Growth of Hollow Hexagonalα-Fe2O3Nanocrystals. Journal of Nanomaterials, 2016, 2016, 1-5.	2.7	2
79	Thermal Expansion and Magnetostriction of Laves-Phase Alloys: Fingerprints of Ferrimagnetic Phase Transitions. Materials, 2019, 12, 1755.	2.9	2
80	Preparation and Characterization of Taxifolin Form II by Antisolvent Recrystallization. Chemical Engineering and Technology, 2019, 42, 414-421.	1.5	2
81	Cobalt vacancies assisted ion diffusion in Co ₂ AlO ₄ carbon nanofibers for enhancing lithium battery performance. Dalton Transactions, 2020, 49, 10127-10137.	3.3	2
82	Giant Vertical Magnetization Shift Caused by Field-Induced Ferromagnetic Spin Reconfiguration in Ni50Mn36Ga14 Alloy. Materials, 2020, 13, 4701.	2.9	2
83	Tuning the exchange bias effect via thermal treatment temperature in bulk Ni ₅₀ Mn ₄₂ In ₃ Sb ₅ Heusler alloys. Applied Physics Express, 2021, 14, 105502.	2.4	2
84	Reduction of Manganese Dioxide by Dissolved Lithium in Liquid Ammonia for Li–Mnâ€O Spinels. ChemistrySelect, 2016, 1, 3438-3442.	1.5	1
85	Experimental Observation of van Hove Singularities in Quasiâ€1D MoO ₂ Nanotubes. Advanced Electronic Materials, 2019, 5, 1900005.	5.1	1
86	The structure, magnetic and magnetocaloric effect of misch-metal (MM)2Fe17â^'xAlx (xÂ=Â0–2) compounds. Journal of Magnetism and Magnetic Materials, 2020, 502, 166487.	2.3	1
87	Anomalous Optically Induced Nonvolatile Magnetization Effect in Mn ₃ O ₄ Superparamagnetic Nanoparticles. Particle and Particle Systems Characterization, 2022, 39, .	2.3	1
88	Influence of measurement field on the magnetic domains for zero-field cooling exchange bias effect in Ni50Mn37Ga13 alloy. Journal of Magnetism and Magnetic Materials, 2022, 553, 169250.	2.3	1
89	Applications of Carbon Nanomaterials in Biosensor. , 2016, , 103-134.		0
90	Removing the surfactant of SmCo5 nanoflakes via ligand-exchange and vacuum heat-treatment. Journal of Magnetism and Magnetic Materials, 2020, 499, 166250.	2.3	0

#	Article	IF	CITATIONS
91	The phase transitions and magnetocaloric effects in Ga-doped Heusler Ni50Mn36Sn14 alloys. Japanese Journal of Applied Physics, 2020, 59, 010905.	1.5	0
92	Multiband transport enables thermoelectric enhancements in the SrMg ₂ Bi ₂ compound. Journal of Applied Physics, 2022, 131, 135101.	2.5	0
93	A three-dimensional crosslinked nano-structure <i>via in situ</i> growth of carbon nanotube/cobalt sulfide composites on porous carbon nanofibers for enhanced sodium storage. Dalton Transactions, 2022, , .	3.3	0
94	Magnetic and Magnetostrictive Behaviors of Laves-Phase Rare-Earth—Transition-Metal Compounds Tb1â^'xDyxCo1.95. Materials, 2022, 15, 3884.	2.9	0